



Numerical study on the propagation of solitary waves in the near-shore

Yanrong Kuai^a, Meilan Qi^{a,b,*}, Jinzhao Li^a

^a School of Civil Engineering, Beijing Jiaotong University, Beijing, 100044, China

^b Beijing Key Laboratory of Structural Wind Engineering and Urban Wind Environment, Beijing, 100044, China

ARTICLE INFO

Keywords:

Wave run-up
Hydrodynamic characteristics
Beach slope
Reynolds-averaged Navier-Stokes equations
Solitary wave

ABSTRACT

The propagation and transformation of water waves in the near-shore region lead complicated wave-current field, which plays a significant role in the study of the mechanism of sediment transport and coastal evolution. Solitary wave is supposed as an initially incoming wave because of its widespread use in the near-shore. The Reynolds-averaged Navier-Stokes (RANS) equations were incorporated into a $k-\epsilon$ turbulence model and applied to simulate the run-up and hydrodynamic characteristics of solitary waves under the influences of different incident wave height and beach slope. The simulation results were validated with theoretical and experimental results from the literature. The effects of the non-linear terms associated with the curl of the fluid, Reynolds stresses and viscous stresses in the governing equations of fluid as well as the turbulent production term, convection term and diffusion term in the $k-\epsilon$ model were analyzed. The analysis shows that wave breaking is of great importance to the hydrodynamic characteristics of the wave-current field in the near-shore. The run-up heights of breaking solitary waves increase with beach slope, and the velocity and vorticity reach the maximum after wave breaking. The non-linear (curl and convection) terms and turbulent production term contribute most to the nonlinearities of the near-shore hydrodynamics, and increase with beach slope under these conditions. Nevertheless, under the conditions of wave non-breaking, the wave run-up height, the maximum of velocity and vorticity decrease with increasing beach slope. Meanwhile, the effects of fluid diffusion and Reynolds stresses increase gradually with increasing beach slope.

1. Introduction

In the process of wave propagation in the coastal region, the wave surface steepens with increasing wave height, and may eventually become unstable and broken. It causes the wave-current field in the near-shore region to become more complicated, which greatly affects the morphological changes of coastal areas and offshore structures (Choi et al., 2015; Kamath et al., 2016). Therefore, it is required to accurately describe the run-up and hydrodynamic characteristics of waves in the process of propagation in the near-shore region.

Wave run-up is one of the important parts of the wave propagation in the near-shore area. Extensive studies on the wave run-up have been reported, including the theories (Synolakis, 1987; Li and Raichlen, 2001; Carrier et al., 2003; Kânoğlu, 2004), experiments (Hsiao et al., 2008; Chang et al., 2009; Sælevik et al., 2013; Drähne et al., 2016) and numerical simulations (Ma et al., 2007; Fuhrman and Madsen, 2008; Chio et al., 2008; Lara et al., 2011; Tsung et al., 2012), which are appropriate for breaking (Ai and Jin, 2012) and non-breaking (Kuiry et al., 2012) waves. Synolakis (1987) proposed a formula to calculate wave run-up height for non-breaking solitary waves based on shallow-

water equations, which indicates that the run-up height decreases with increasing beach slope. However, the calculated results are larger than the measured values (Sriram et al., 2016). Li and Raichlen (2001) proposed a nonlinear theoretical solution for wave run-up using the Carrier and Greenspan (1958) transformation, and the calculation results are better than that obtained by Synolakis (1987). The run-up height of the breaking wave is different from that of the non-breaking wave (Synolakis, 1987). Hsiao et al. (2008) indicated that the run-up height increases with beach slope for breaking solitary waves. The breaking criterion plays a significant role in the calculation of wave run-up height. Many studies have attempted to define breaking criteria for solitary wave run-up on plane slopes (Camfield and Street, 1969; Synolakis, 1986; Grilli et al., 1997). Synolakis (1986) predicted much smaller wave height for breaking on a given slope. Grilli et al. (1997) developed the breaking criteria based on the potential equations. However, some non-linear terms are neglected, which may be not appropriate in some certain conditions (Qi et al., 2017).

It is necessary to study the hydrodynamic characteristics before and after wave breaking in the process of wave propagation under different conditions (Chen et al., 2011; Peregrine and Williamss, 2001; Pringle

* Corresponding author. School of Civil Engineering, Beijing Jiaotong University, Beijing 100044, China.

E-mail address: mlqi@bjtu.edu.cn (M. Qi).

et al., 2016). Li and Raichlen (2002) found that the energy dissipation is closely associated with wave breaking. Mo (2013) focused on the wave transformation and the characteristic of velocity field in the wave propagation. Hsieh (2016) studied the spatial variation of the hydrodynamic factors, including vorticity, convection term and turbulent production term. However, the influence of the beach slope on the wave transformation and hydrodynamic characteristics in the near-shore area was not concerned.

This study presents the numerical investigations of the run-up and hydrodynamic characteristics of solitary waves influenced by the incident wave height and beach slope. The unsteady Reynolds-averaged Navier-Stokes (RANS) equations coupled with a $k-\epsilon$ turbulence model are applied to simulate the wave run-up on beach slopes. Then the evolution of the velocity field and vorticity in the wave propagation are studied. Furthermore, the effects of the beach slope on the nonlinear terms in the RANS equations and $k-\epsilon$ model are analyzed.

2. Numerical model

2.1. Governing equations

Wave deformation, wave breaking and wave-induced current in the near-shore play important roles on the coastal topography evolution and offshore engineering, on which a lot literature discussed using non-potential flow models (Choi et al., 2008; Lara et al., 2011; Smit et al., 2013). Solitary wave in the near-shore approaching to and climbing up the sloped beach, the wave front becomes steeper, and eventually the wave breaks. In this process, the velocity gradient becomes strong and the effects of viscosity and curl of the fluid play an important role in the near-shore. Therefore, the unsteady Reynolds-averaged Navier-Stokes (RANS) equations, calculating the time-averaged components of the flow, are used to simulate the propagation of solitary waves on a uniform sloping beach in a two-dimensional fluid domain. The governing equations for an incompressible fluid are expressed as follows:

$$\text{Continuity equation: } \frac{\partial u_i}{\partial x_i} = 0 \quad (1)$$

$$\text{Momentum equation: } \frac{\partial u_i}{\partial t} + u_j \frac{\partial u_i}{\partial x_j} = -\frac{1}{\rho} \frac{\partial p}{\partial x_i} + g_i + \frac{\partial}{\partial x_j} \left(\nu \frac{\partial u_i}{\partial x_j} - \overline{u_i u_j} \right) \quad (2)$$

where i and j are the cyclic coordinates in an orthogonal coordinate system whose values are 1 and 2, while u_i are the time-averaged velocity components; ρ is the density of the fluid; p is the pressure; g_i is the gravitational acceleration; $-\overline{u_i u_j}$ denotes the turbulent Reynolds stresses which can be expressed as $-\overline{u_i u_j} = \nu_t (\partial u_i / \partial x_j + \partial u_j / \partial x_i) - 2/3 k \delta_{ij}$, where ν_t is the turbulence eddy viscosity. In this study, ν_t is simulated using the standard $k-\epsilon$ turbulence model proposed by Launder and Spalding (1974), which are as following:

$$\frac{\partial k}{\partial t} + u_j \frac{\partial k}{\partial x_j} = \frac{\partial}{\partial x_j} \left[\left(\frac{\nu_t}{\sigma_k} + \nu \right) \frac{\partial k}{\partial x_j} \right] + G - \epsilon \quad (3)$$

$$\frac{\partial \epsilon}{\partial t} + u_j \frac{\partial \epsilon}{\partial x_j} = \frac{\partial}{\partial x_j} \left[\left(\frac{\nu_t}{\sigma_\epsilon} + \nu \right) \frac{\partial \epsilon}{\partial x_j} \right] + C_{1\epsilon} \frac{\epsilon}{k} G - C_{2\epsilon} \frac{\epsilon^2}{k} \quad (4)$$

where five related coefficients suggested by the original author are utilized: $C_{1\epsilon} = 0.09$, $C_{2\epsilon} = 1.44$, $C_{3\epsilon} = 1.92$, $\sigma_k = 1.0$, $\sigma_\epsilon = 1.3$.

2.2. Computational domain setting, initial and boundary conditions

2.2.1. Computational domain setting

The computational domain for the propagation of solitary waves in the near-shore area is shown in Fig. 1, in which the seabed is simplified to a uniform slope. In the figure, H is the incident wave height; h is the

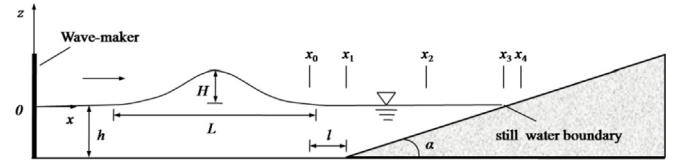


Fig. 1. Sketch of the calculation model.

still water depth at the plane bed; L is the wave length; α is the angle of beach slope; x , z are the horizontal and vertical coordinates, respectively.

2.2.2. Initial and boundary conditions

In the computational domain, the piston-type wave-maker is located on the left and the nonlinear algorithms developed by Goring (1978) are used to generate solitary waves. The origin of coordinates is located at the still water surface on the left, and the wave propagates from left to right. The boundaries of the computational domain include the free surface on the top, a solid no-slip wall at the bottom and on the right. At the initial time, the water velocities in the whole computational zone are set to zero.

2.2.3. Mesh description

The quadrilateral grids are used in the simulation and are parallel to the bottom, as shown in Fig. 2. The influence of grid size on the computational results was investigated. We tested three different meshes with different uniform grid sizes, which are defined as M1, M2 and M3. The detailed information on meshes and computational results are shown in Table 1. In contrast to solitary waves on slopes (Chang et al., 2009), the computed wave surface elevations with the coarsest grid (M1) are generally smaller than the experimental results. The numerical results of M2 and M3 are closer to the experimental results. To balance the calculation precision and speed, the mesh size of $\Delta x = \frac{L}{290}$ and $\Delta y = \frac{H}{17}$ (M2) is adopted. The optimization of the time step, Δt , is subject to the Courant number constraint $Cr = \sqrt{gh} \Delta t / \Delta x < 1$.

2.3. Numerical schemes and model validation

2.3.1. Numerical schemes

Eqs. (1) and (2) are solved numerically by a two-step projection method with finite volume spatial discretization (Issa, 1986). The linear least square reconstruction method is adopted to evaluate gradients at cell centers (Barth, 1992). Time derivative is discretized by the forward time difference method. First and second-order accuracy is obtained for the temporal and spatial terms, respectively.

The volume of fluid (VOF) method is employed for tracing or capturing the free surface (Hirt and Nichols, 1981). The governing equation is as follows:

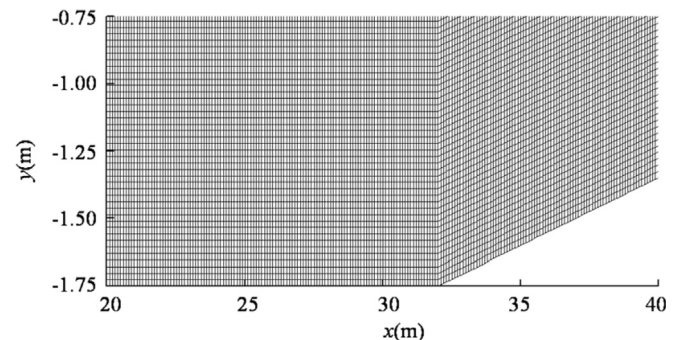


Fig. 2. Diagram of mesh ($H/h = 0.235$).

Download English Version:

<https://daneshyari.com/en/article/8061765>

Download Persian Version:

<https://daneshyari.com/article/8061765>

[Daneshyari.com](https://daneshyari.com)